inter.noise
HAMBURG 2016

Turbulent boundary layer noise in pipe flow

Seung Tae Hwang[1,a)] and Young J. Moon[1,b)]

Computational Fluid Dynamics and Acoustics Laboratory

School of Mechanical Engineering

Korea University

Seoul, 136-701 Korea, Rep. of

ABSTRACT

Turbulent boundary layer noise in pipe flow at $Re_D = 5000$ (or $Re_\tau = 175$) and M = 0.1 is investigated by a LES/LPCE hybrid method. The generation and propagation of acoustic waves are computed by solving the linearized perturbed compressible equations (LPCE), with acoustic sources ($\mathrm{DP(x,t)/Dt}$) attained by incompressible large eddy simulation (LES). The acoustic power spectral density is closely compared with the wall shear-stress fluctuation dipole source of the turbulent channel flow at $Re_\tau = 180$ [Hu, Morfey, and Sandham [4]. A constant decaying rate of - 8/5 in the power spectrum is found to be related to turbulent bursts of coherent structures such as hairpin vortex and their merged structures (or hairpin packets), in particular, to their streamwise length scales that represent indeed the local rate of changes of the streamwise linear momentums.

Keywords: TBL noise, turbulent pipe flow
I-INCE Classification of Subjects Number(s): 21.6.4

1. INTRODUCTION

Turbulent boundary layer noise has been considered an important issue in turbulent flow research for several decades. It is one of the design variables to be controlled in aircraft industries or companies of power plants with ducts, since noise can significantly be transmitted through the walls. Recently lives have been more indoor-centered due to increased industrial dusts and dirts of fine particles. Thus office buildings and residential houses are more demanded to be equipped with air-conditioners run by high-powered duct flows and noise is now an unavoidable issue.

The sound generated in the turbulent boundary layer (called TBL noise hereafter) can be either transmitted through the duct walls, or propagate inside the ducts. The noise transmission through the wall occurs via acoustic loading or wall pressure fluctuations by local convecting near-wall turbulences. Even though the energy level of the acoustic loading is much lower than that of wall pressure fluctuations, its transmission can be comparable when a transfer function is considered.

A main concern of duct flow noise is the noise transmission at low wavenumbers since it is more likely to interact with structures by resonance. On the low wavenumber acoustics, a few but very intensive theoretical studies have been conducted since 1950's; the Kraichnan-Phillips theorem asserted that the wall pressure fluctuation spectrum converges to zero in a sub-convective region (i.e. axial wavenumber is less than ω/U_∞ but still larger than ω/c. Including the compressibility effect, Ffowcs-williams [1] showed later in his theoretical work that the spectral levels of the wall pressure fluctuation at the sub-convective and acoustic regions must have a finite non-zero value. Recent works of experimental measurement [2] and direct compressible Navier-Stokes computations [3] also showed that the compressibility effect is essential when the low wavenumber spectral contribution is concerned.

To reduce the transmitted noise generated in the sub-convective region, it is important to characterize the near-wall turbulences; to be more specific, which structures with what length scales

[1,a)] seungtae05@korea.ac.kr, Graduate student
[1,b)] yjmoon@korea.ac.kr, Corresponding author

and time scales are more actively participating in the generation of TBL noise. Hu et al.[4] quantified the TBL noise sources in turbulent channel flow with the incompressible direct numerical simulation (DNS) and applied the Lighthill's acoustic analogy to predict the power spectrum of the far field pressure fluctuations at low Mach numbers. They found that the acoustic pressure fluctuation of the dipole source was dominant below a specific Mach number (e.g. M < 0.1). Arguillat et al.[2] also measured the wall pressure fluctuations in turbulent channel flow at low Mach numbers, and showed that when the noise transmission is included in the analysis, not only the aerodynamic loading by hydrodynamic pressure but also the effect of the low wavenumber (acoustic part) have to be taken into account.

One of the main objectives of the present study is to understand the noise generation mechanisms in turbulent pipe flow at low Mach numbers. To examine the near-wall turbulence structures and their dynamics, incompressible large eddy simulation (LES) is conducted for $Re_D = 5000$ in a computational domain of 22 pipe diameters in the streamwise direction. The acoustic field at M = 0.1 is directly computed by solving the linearized perturbed compressible equation (LPCE), with acoustic source, DP/Dt acquired from the incompressible LES solution. The computed acoustic power spectrum is analyzed in discussion with the acoustic source models proposed by Morfey in 1973[5], in particular, the acoustic dipole with wall shear-stress fluctuations.

This paper is organized as follows. In Sec. 2, the computational methodology of the present study is described. The computational details, LES field results and turbulent statistics are discussed in Sec. 3. Sec. 4 firstly introduces the new noise modeling procedure based on the LES/LPCE hybrid method and explains the acoustic modeling results using consecutive field solutions of LPCE. Then, additional analysis related to the TBL noise generation is carried out. Finally, the paper provides its conclusion in Sec. 5.

2. LES/LPCE HYBRID FORMULATION

The present LES/LPCE hybrid method is based on a hydrodynamic/acoustic splitting method (Hardin et al.[6]), in which the total flow variables are decomposed into the incompressible and perturbed compressible variables as,

$$\begin{aligned} \rho(\vec{x},t) &= \rho_0 + \rho'(\vec{x},t) \\ \vec{u}(\vec{x},t) &= \vec{U}(\vec{x},t) + \vec{u}'(\vec{x},t) \\ p(\vec{x},t) &= P(\vec{x},t) + p'(\vec{x},t) \end{aligned} \tag{1}$$

The incompressible variables represent the hydrodynamic flow field, while the acoustic fluctuations and other compressibility effects are resolved by the perturbed quantities denoted by (').
The hydrodynamic turbulent flow field is first solved by incompressible LES. The filtered incompressible Navier-Stokes equations are written as,

$$\frac{\partial \widetilde{U_j}}{\partial x_j} = 0 \tag{2}$$

$$\rho_0 \frac{\partial \widetilde{U_i}}{\partial t} + \rho_0 \frac{\partial}{\partial x_j}\left(\widetilde{U_i}\widetilde{U_j}\right) = -\frac{\partial \tilde{P}}{\partial x_i} + \mu_0 \frac{\partial}{\partial x_j}\left(\frac{\partial \widetilde{U_i}}{\partial x_j} + \frac{\partial \widetilde{U_j}}{\partial x_i}\right) - \rho_0 \frac{\partial}{\partial x_j} M_{ij} \tag{3}$$

where the grid-resolved quantities are denoted by $(\sim)$ and the unknown sub-grid tensor M_{ij} is modeled as

$$M_{ij} = \widetilde{U_i U_j} - \widetilde{U_i}\widetilde{U_j} = -2(C_s\Delta)^2 \left|\tilde{S}\right| \widetilde{S_{ij}} \tag{4}$$

Here, Δ is the mean radius of the grid cells (computed as cubic root of its volume), and $\widetilde{S_{ij}}$ is the strain-rate tensor.

After a quasi-periodic stage of the hydrodynamic field is attained, the perturbed quantities are computed by the linearized perturbed compressible equations (LPCE)(Seo et al.[7]). A set of the linearized perturbed compressible equations is written as,

$$\frac{\partial \rho'}{\partial t} + \left(\vec{U} \cdot \nabla\right)\rho' + \rho_0(\nabla \cdot \vec{u}') = 0 \tag{5}$$

$$\frac{\partial u'}{\partial t} + \nabla\left(\vec{u}' \cdot \vec{U}\right) + \frac{1}{\rho_0}\nabla p' = 0 \tag{6}$$

$$\frac{\partial p'}{\partial t} + \left(\vec{U} \cdot \nabla\right)p' + \gamma P(\nabla \cdot \vec{u}') + (\vec{u}' \cdot \nabla)P = -\frac{DP}{Dt} \tag{7}$$

The left hand side of LPCE represents effects of acoustic wave propagation and refraction in an unsteady, inhomogeneous flow, while the right hand side only contains an explicit acoustic source component, which is projected from the incompressible LES flow solution. It is interesting to note that for low Mach number flows, the total derivative of the hydrodynamic pressure, DP/Dt is only considered as the explicit noise source term. From the curl of linearized perturbed momentum equations, Eq.(6) yields

$$\frac{\partial \vec{\omega}'}{\partial t} = 0 \tag{8}$$

The LPCE prevents any further changes (generation, convection and decaying) of perturbed vorticity in time, In fact, the perturbed vorticity could generate self-excited errors if ω' is not properly resolved with the acoustic grid. Hence, the evolution of the perturbed vorticity is pre-suppressed in LPCE, deliberating the fact that the perturbed vorticity has little effects on noise generation, particularly at low Mach numbers. For the hybrid method, this is an important property that ensures consistent, grid-independent acoustic solutions. Derivation of LPCE and the detailed discussion on characteristics of the perturbed vorticity can be found in Seo et al.[7].

The filtered incompressible Navier-Stokes equations are solved by an iterative fractional-step method (Poisson equation for the pressure), wheras the linearized perturbed compressible equations are solved in a time-marching fashion. To avoid excessive numerical dissipations and dispersions errors, the governing equations are spatially discretized with a sixth-order compact finite difference scheme (Lele [8]) and integrated in time by a four-stage Runge - Kutta method.

Practically, when a high order scheme is applied to stretched meshes, numerical instability is encountered due to numerical truncations or failure of capturing high wave-number phenomena. Thus, a tenth-order spatial filtering (cut-off wavenumber, $k\Delta x \approx 2.9$) proposed by Gaitonde et al.[9] is applied to every iteration to suppress the high frequency errors that might be caused by grid non-uniformity. For the far-field boundary condition, the energy transfer and annihilation (ETA) boundary condition (Edgar et al.[10]) with a buffer zone is used for eliminating any reflection of the out-going waves. The ETA boundary condition is easily facilitated with a rapid grid stretching in the buffer-zone and spatial filtering which damp out waves shorter than grid spacing. Therefore, if the buffer-zone has a grid spacing larger than the out-going acoustic wave length, the wave can be successfully absorbed by the ETA boundary condition.

3. LARGE EDDY SIMULATION OF TURBULENT PIPE FLOW

For a computation of turbulent pipe flow, an incompressible large-eddy simulation is first intended to be conducted with periodic boundary condition imposed in the streamwise direction. According to recent experimental studies (Kim et al.[11]), however, very large and large-scale motions (VLSM and LSM) with lengths of 5R up to 20R (R is the pipe radius) have been observed in the outer region of the

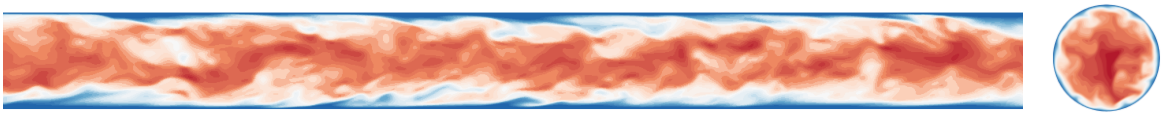

(a) (b)

Figure 1 - Turbulent pipe flow in the first half of the computational domain $0 \leq z \leq 11D$, (a) constant θ-plane of streamwise velocity u_z' (b) constant z-plane of streamwise velocity u_z'.

turbulent boundary layer in a fully-developed pipe flow. Recent numerical studies have also been conducted with a computational domain large enough to resolve such large scale turbulent motions. For example, Wu et al.[12] used the computational domain of 30R as in the DNS study to analyze the (very) large scale motions at $Re_\tau = 685$. Chin et al.[13] also carried out a DNS study at $Re_\tau = 170$ and 500 to investigate the effect of the streamwise periodic length on the convergence of turbulence statistics and concluded that the corresponding streamwise domain length of convergence was achieved with 8R.

The present study is focused not only on the turbulent pipe flow modeling but also on generation and propagation of the acoustic field. Therefore, a computational domain used in this study is large enough (22D, D is the pipe diameter) to analyze the effect of the flow and acoustics at the same time. The Reynolds number based on the pipe diameter $Re_D = 5000$ and the friction Reynolds number (also known as Karman number) $Re_\tau = R^+ = u_\tau R/\nu = 175$ are used in the present simulation. The computational grid size is $120 \times 241 \times 1560$ (about 45 millions) along r, θ, and z directions, respectively. The grid resolution along the axial direction is $\Delta z^+ = 5.6$ (or $\Delta z = 3.5 \times 10^{-5}$). Along the azimuthal direction, the maximum grid spacing is $R\Delta\theta^+ = 4.55$ (or $R\Delta\theta = 2.8 \times 10^{-5}$) at the pipe wall (r = R). The minimum and maximum wall-normal grid spacings are $= 2.2 \times 10^{-6}$ and 1.76×10^{-5}, respectively and in a wall unit, these correspond to 0.35 and 2.8.

The incompressible LES was conducted with 600 processors of SUN B6275 at the KISTI supercomputer center located in Daejun, Korea, Rep. of. Both LES and LPCE calculations use same time step in this simulation with the CFL number chosen as 0.58 (or $\Delta t^+ = 9.6 \times 10^{-5}$), and the total simulation time is about $700R/U_\infty$. A statistical sampling is conducted in two homogeneous directions (θ, z). The fully-developed turbulent pipe flow is presented in Figure 1 by the flooded contours of the instantaneous streamwise velocity at a constant θ-plane(a) and a constant z-plane(b). A total of 30 contour levels are used to depict the magnitude of u_z' from 0.004 (blue) to 1.4 (red), visualizing the turbulent eddy structures in the pipe.

The present LES is validated by comparing with the existing DNS solutions of Khoury et al.[14], who studied the characteristics of turbulent pipe flow in a smooth circular pipe of axial length 25R at $Re_D = 5300$. The inner-scaled mean velocity profile of the present calculation is well compared in Figure 2 with the DNS result. In Figure 3(a), the three components of turbulence intensity, $u'_{z,rms}$, $u'_{\theta,rms}$ and $u'_{r,rms}$ are also quite closely compared with those of DNS, even in the second-order turbulence statistics. However, another second-order statistics representing the turbulent shear stress shows some slight discrepancies in Figure 3(b). Such difference seems to occur due to grid resolution or Reynolds number disparity. Nevertheless, the turbulent motions seem well reflected on the first and second-order statistics

A power spectral density of the hydrodynamic wall pressure fluctuation computed from incompressible LES is scaled with an inner flow variable and presented in Figure 4, in comparison with the DNS data of Gloerfelt and Berland[3] for a subsonic flow over a flat plate (Re_θ = 1491 and M = 0.5). It is interesting to note that the hydrodynamic wall pressure fluctuations for an internal turbulent boundary layer is quite closely compared with those for an external turbulent boundary layer, meaning that those turbulent eddies exchanging the normal momentums with the wall exhibit similar dynamic characters.

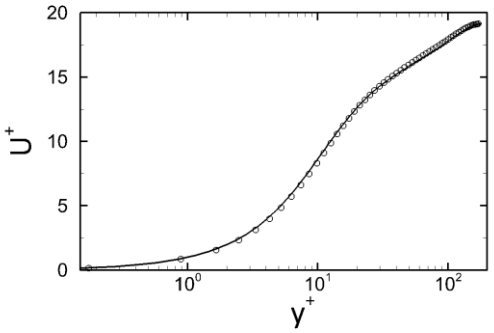

Figure 2 - Mean axial velocity U^+ as a function of y^+. circles: present LES at $Re_D = 5000$; solid line:

Khoury et al.[14] at $\mathrm{Re_D} = 5300$.

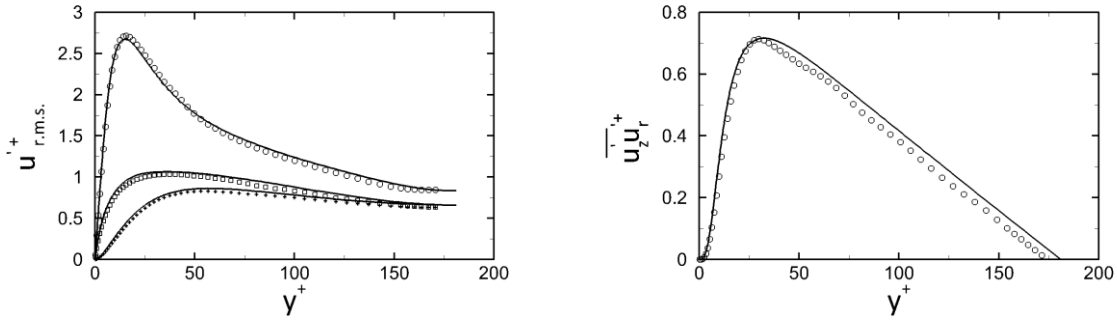

(a) (b)

Figure 3 - (a) Turbulence intensity u'_{rms} vs. y^+; present LES ($Re_D = 5000$): $u'_{z,rms}$ (circle), $u'_{\theta,rms}$ (square), $u'_{r,rms}$ (cross); Khoury et al.[14]: line ($Re_D = 5300$), (b) Turbulent shear stress $\overline{u'_z u'_r}$ vs. y^+; present LES: circle; Khoury et al.[14]: line.

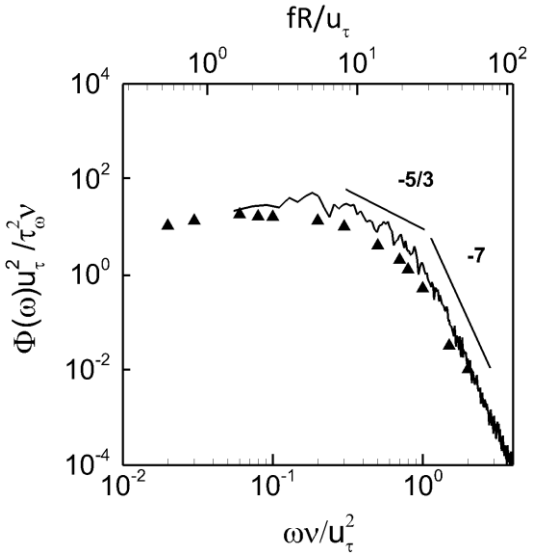

Figure 4 - Point spectra of wall pressure fluctuation. solid line: present LES; ▲: Turbulent boundary layer DNS, Re_θ = 1491(Gloerfelt and Berland[3]).

4. ACOUSTICS OF TURBULENT PIPE FLOW

4.1 Acoustic Field Prediction Method

In the present study, two different computational domains are configured as in Figure 5 to separate incompressible LES and LPCE computations.

The computational domain for LPCE is complicated than that for LES to include not only the acoustic source region but also the zones for source filtering, data collecting, and wave annihilation. The specific grid resolution in LPCE is consistent with LES calculation except for streamwise direction in both end boundaries to prevent any wave reflection. The source filtering zone, enclosing the noise source zone eliminates the fluctuating acoustic source factors such as velocity and the hydrodynamic pressure. Both the time and spatial evolutions of the acoustic waves generated by turbulent flow in source region are gathered in the acoustic monitoring zone. The acoustic annihilating zone, located at both ends of the computational domain gradually eliminates the acoustic pressure propagation with the extended grids. 50 grid points are distributed for 100D (D = pipe diameter) along the axial direction to prevent any wave reflections from the ends. The LES results used in both the acoustic monitoring and the acoustic annihilating zone are same as that used in the source filtering zone in which the fluctuating components are gone to prevent additional noise generation.

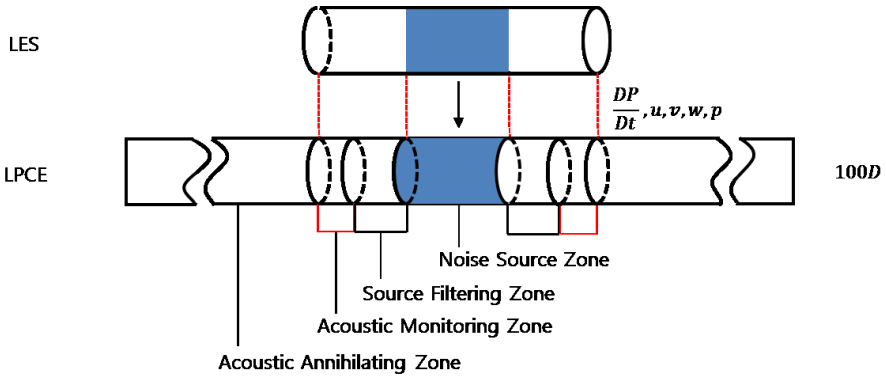

Figure 5 - Schematic of turbulent pipe flow noise prediction method

4.2 Acoustic Field

An LPCE prediction for acoustic field was conducted in conjunction with LES. A three-dimensional shaded view of the compressibly perturbed pressure fluctuations (p') at a constant θ-plane is presented in Figure 6 to visualize the instantaneous compression and expansion states of the waves. Five consecutive images with a time interval of $\Delta t = 0.28\ D/U_\infty$ show not only the hydrodynamic pressure fluctuations by turbulences but also the spatial formation and propagation of the acoustic waves. One can clearly note that two noticeable acoustic waves propagate towards both ends of the computational domain inside the pipe and that the convection speed of the continuous field solutions corresponds to the speed of sound.

In a circular pipe, acoustic mode is determined by a cut-off frequency of higher modes, $f_{m,n} = n_{m,n}c/(2\pi R)$ where $n_{m,n}$ calculated from the Helmholtz equation denotes a number of nodal lines in the radial and azimuthal directions, respectively, with c being the speed of sound and R the pipe radius. For the computed acoustic field, acoustic mode is therefore checked to see the evanescence of the acoustic waves at the far field. The higher acoustic modes can be checked by phase angles at a cross-section of the pipe. Using the time evolution of acoustic pressure from a plane in the acoustic monitoring zone, the phase analysis is conducted with equally-distributed 30 points in both radial and azimuthal directions. As presented in Figure 7, a non-zero phase angle is only visible at the frequency close to 1.55 in terms of inner variables, and it is indeed close to the analytical cut-off frequency of (1,0) mode, that is,1.6. In other words, there is no clear tendency of an additional acoustic mode at higher frequency, implying that the (1,0) mode is only observed in the present study. The phase angles near the (1,0) cut-off frequency range from - 90 ~ 90 degrees, with maximum and minimum at the pipe circumference. This is consistent with a representative characteristic of the acoustic higher mode, known as the spiral wave motion. There is, however, no clear higher acoustic modes, implying that acoustic waves at higher frequencies are expected to be either quickly damped by decaying characteristics of the small-scale turbulences or evanescence of waves during transmission in the pipe.

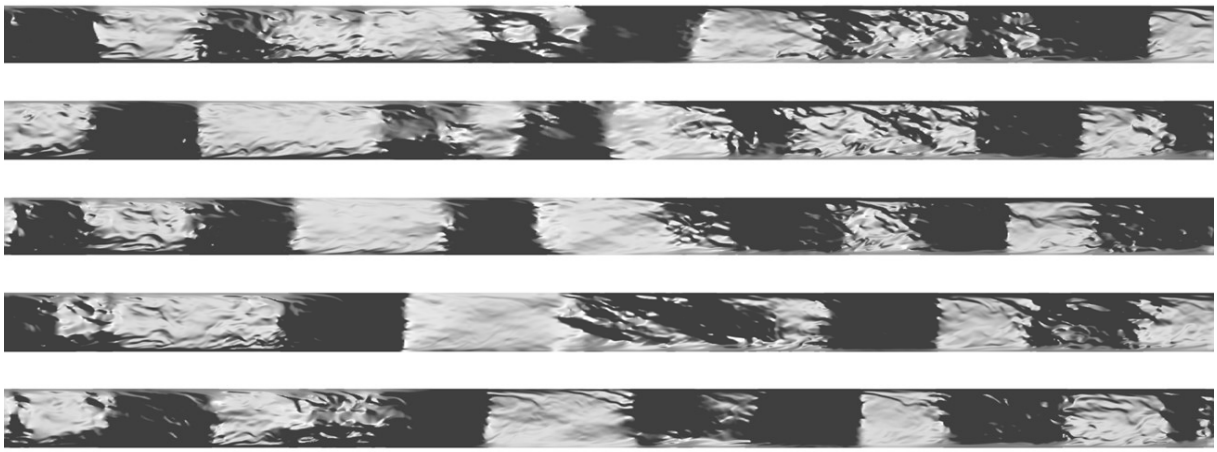

Figure 6 - Time series of compressibly-perturbed pressure fluctuation field with a time interval ($\Delta t = 0.28\ D/U_\infty$) at a constant θ-plane.

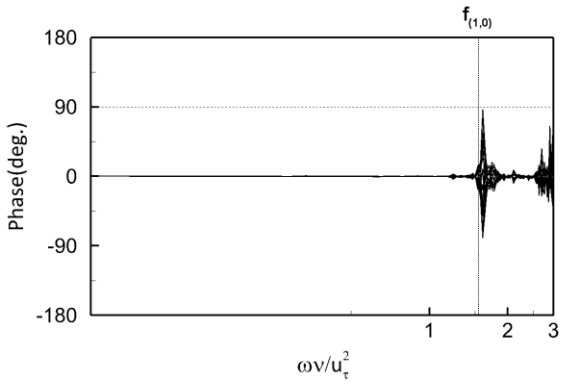

Figure 7 - Phase angle analysis. dashed line: analytic (1,0) duct mode frequency.

A power spectral density of acoustic pressure computed by the present LES/LPCE method is compared in Figure 8 with the acoustic dipole source (marked by ▲), attained by incompressible DNS for a turbulent channel flow at $Re_\tau = 180$ (Hu et al.[4]). As pointed out by Hu et al.[4], the TBL noise generation at low Mach number (e.g. M < 0.1) is majorly attributed to the linear mode conversion from incident vorticity wave to the pressure wave near the solid boundary. This noise mechanism was initially mentioned from Herbert, Leehay and Haj-Hariri[15], and similar to that of elastodynamics with respect to mode conversation from shear to dilatational wave. The axial dipole source (S11) spectrum of Hu et al.[4] scaled by $(S_p(f)Re_\tau)$ shows good agreement with the LPCE result from low to mid-range frequencies (fR/u_τ < 10). The spectral difference in high frequencies (10 < fR/u_τ < 20) may be explained by missing contributions from the quadrupole and monopole sources. Nevertheless, the agreement is quite self-evident.

The main mechanism of TBL noise generation eventually belongs to the vorticity scattering, consistent with the scattering in trailing edge by surface roughness element. A constant decaying rate of acoustic power spectrum in turbulent pipe flow is considered to be closely related to turbulent bursts of coherent structures such as hairpin vortex and their merged structures (or hairpin packets), in particular, to their streamwise length scales that represent indeed the local rate of changes of the streamwise linear momentums, i.e.

$$p'_a \propto \rho_\infty l^\beta \left(\frac{\partial u_z}{\partial t}\right) \tag{9}$$

where l denotes a longitudinal correlation length scale and $\beta \cong 1$. With the fact that the local rate of

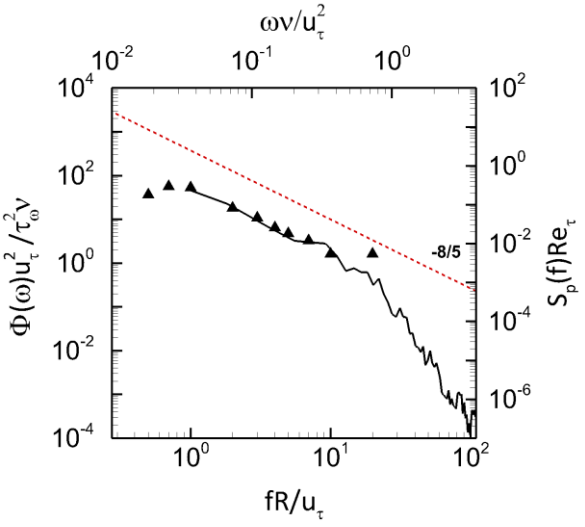

Figure 8 - Point spectra of acoustic pressure fluctuation with acoustic source spectra. solid line: acoustic pressure, symbol: acoustic source (streamwise dipole).

change of the streamwise linear momentum is nearly constant regardless of its correlation length scale and with the Taylor's hypothesis ($l \cdot f = 0.83U_\infty$), the acoustic pressure is again written as

$$p'_a \propto f^{-\beta} \tag{10}$$

and so $[p'_a]^2 \propto f^{-2\beta}$. Note that β is less than 1 for eddies convecting in TBL since the longer the streamwise correlation length of hairpin or its packets, the less coherent its local rate change of the streamwise momentum. For example, if β = 4/5, then $[p'_a]^2 \propto f^{-8/5}$. The decaying slope β has to be more scrutinized for different Reynolds numbers and Mach numbers.

5. CONCLUSIONS

The noise generation by a turbulent pipe flow was analyzed by a hybrid LES/LPCE method to tackle an acoustic problem at a low Mach number. The acoustic field was determined by solving the linearized perturbed compressible equations (LPCE) based on the source term $(DP(x,t)/Dt)$ obtained by the incompressible large eddy simulation (LES).

The LES domain extends in the longitudinal direction to 22D (D, pipe diameter) to examine the noise source contribution of the near-wall turbulent structures to the acoustic field. The Reynolds number was $Re_\tau = 175$ and the Mach number M = 0.1. The turbulent statistics and the power spectrum of the wall pressure fluctuations showed a good agreement with the findings of the previous DNS solutions. The phased analysis of the acoustic results showed that the duct mode at (1,0) possesses a spiral wave motion. Furthermore, the auto-correlation of the acoustic pressure signal identified the dipole source induced by the wall shear stress distribution.

The TBL noise in the pipe flow is caused by the acoustic scattering of the vortex source, consistent with the scattering in trailing edge. The noise generation in pipe is conjectured that the pressure fluctuation in the burst-phase inside the turbulence boundary layer is related with the rate of the linear momentum change $(p'_{acou} \propto \rho_\infty l \frac{\partial u_z}{\partial t})$. In the present analysis the magnitude of the acoustic pressure fluctuation was proportional to the turbulent correlation length in longitudinal direction which leads the spectral slope $(f^{-8/5})$ of acoustic pressure fluctuation.

ACKNOWLEDGEMENTS

This work was supported by the HPC Applied Research Supporting Program (No. KSC-2013-G2-004) from KISTI Supercomputing Center, Korea. The authors would like to thank their consideration.

REFERENCES

1. J. E. Ffowcs Williams "Surface pressure fluctuations induced by boundary layer flow at finite Mach number," J. Fluid Mech. 22, 507-519 (1965).
2. B. Arguillat, D. Ricot, C. Bailly, G. Robert. "Measured wavenumber: frequency spectrum associated with acoustic and aerodynamic wall pressure fluctuations," J. of Acoustical Society of America 128, 4, 1647-1655 (2010).
3. X. Gloerfelt, J. Berland "Turbulent boundary layer noise: direct radiation at Mach number 0.5," J. Fluid Mech. 723, 318-351 (2013).
4. Z. W. Hu, C. L. Morfey, N. D. Sandham "Sound radiation in turbulent channel flows," J. Fluid Mech. 475, 269-302 (2003).
5. C. L. Morfey, "Amplification of aerodynamic noise by convected flow inhomogeneities," J. Sound Vib. 31, 391-397 (1973).
6. J. C. Hardin, D. S. Pope, "An acoust/viscous splitting technique for computational aeroacoustics," Theoretical Computational Fluid Dynamics 6, 323-40 (1994).
7. J. H. Seo, Y. J. Moon, "Linearized perturbed compressible equations for low Mach number aeroacoustics," J. Computational Physics 218, 702-719 (2006)
8. S. K. Lele, "Compact finite difference schemes with spectral like resolution,' J. Computational Physics 103, 16-42 (1992).
9. D. Gaitonde, J. S. Shang, J. L. Young, "Practical aspects of high order numerical schemes for wave propagation phenomena," Int J. Numer Methods Engineering 45, 1849-69 (1992).

10. N. B. Edgar, M. R. Visbal, "A general buffer zone type non reflecting boundary condition for computational aeroacoustics," AIAA Paper 3240, (2003)
11. K. C. Kim, R. J.~] Adrian, "Very large-scale motion in the outer layer," Physics of Fluids 11, 2 417-422 (1999).
12. X. Wu, J. R. Baltzer, R. J. Adrian, "Direct numerical simulation of a 30R long turbulent pipe flow at R^+ = 685: large- and very large-scale motions," J Fluid Mech. 698, 235-281 (2012).
13. C. Chin, A. S. H, Ooi, I. Marusic, H. M. Blackburn "The influence of pipe length on turbulence statistics computed from direct numerical simulation data," Phys. Fluids 22, 115107 (2010).
14. G. K. E. Khoury, P. Schlatter, A. Noorani, P. F. Fischer, G. Brethouwer, A. V. Johansson, "Direct numerical simulation of turbulent pipe flow at moderately high Reynolds numbers," Flow Turbulence Combustion 91, 475-495 (2013).
15. K. Herbert, P. Leehey, H. Haj-hariri "On the Mach- and Reynolds-number dependence of the flat-plate turbulent boundary layer wall-pressure spectrum," Theor. Comput. Fluid Dyn. 13, 33-56 (1999).